Lamellar Orientation in Transcrystalline γ Isotactic Polypropylene Nucleated on Aramid Fibers

E. Assouline,*,†,‡ E. Wachtel,§ S. Grigull,⊥ A. Lustiger,# H. D. Wagner,‡ and G. Marom†

Casali Institute of Applied Chemistry, Edmond Safra Campus, Givat Ram, The Hebrew University of Jerusalem, Jerusalem 91904, Israel; Department of Materials and Interfaces, The Weizmann Institute of Science, Rehovot 76100, Israel; Chemical Services Unit, The Weizmann Institute of Science, Rehovot 76100, Israel; ESRF, BP 220, F-38043 Grenoble Cedex, France; and ExxonMobil Research and Engineering, Route 22 East, Annandale, New Jersey 08801

Received August 6, 2001; Revised Manuscript Received October 27, 2001

ABSTRACT: γ orthorhombic isotactic polypropylene transcrystallinity nucleated on aramid fibers under high pressure was investigated by synchrotron X-ray diffraction and by scanning electron microscopy. It was determined that the *c* axes of the lamellae (the growth axes) are distributed radially about the fiber and that the lamellar *ab* face is randomly oriented on the fiber surface. This finding is consistent with the apparent absence of an epitaxial relationship between the crystal structure of the surface of the Kevlar aramid fiber and the lattice of γ iPP crystals.

Introduction

The morphology of interfacial transcrystallinity developed between a reinforcing fiber and a polymer matrix differs significantly from that of polymer crystals in the bulk due to the high density of heterogeneous nucleation sites at the fiber surface. Though epitaxy is not a necessary condition for nucleation, as evidenced by the large variety of nucleating agents, it does occur often for transcrystallization on fiber substrates. Epitaxy involves the oriented overgrowth of one crystal on another and the parallelism of the two crystal lattice planes that have nearly identical arrangements of atoms.[1] In the case of polyethylene/polyethylene composites epitaxy can occur due to the obviously favorable lattice match.[2] It was also found that Kevlar and pitch-based carbon fibers induce transcrystallization of poly(ether ketone ketone), poly(ether ether ketone), and poly(phenyl sulfide) because of an epitaxial effect.[3]

In the case of isotactic polypropylene (iPP) as the matrix, the transcrystalline morphology is potentially complex because of the polymorphic nature of the polymer and the possibility of branching. As reported in previous studies, the transcrystalline (tc) layer may consist of purely α (monoclinic)[4,5] or a mixture of the α and β (trigonal) phases.[6,7] Recently, a mixture of α and γ (orthorhombic) transcrystallinity was obtained by inserting a high weight fraction of high modulus carbon fibers or Kevlar 49 aramid fibers in iPP,[8] and a pure γ tc layer could be generated using a high-pressure crystallization cell.[9] High spatial resolution X-ray diffraction has been shown to be a useful tool for obtaining details of the morphology of α iPP transcrystallinity.[4] It was demonstrated that the parent lamellae nucleate at the surface of a Kevlar fiber with the *c* axes of the crystallites (and thus the polymer chains) parallel to the fiber axis, twist one-quarter turn about the radially directed parent *a** axes within an approximate distance of 25 μm, and then continue to grow without further twisting. This model also includes a characteristic feature that was established for α spherulites: the homoepitaxy of the *ac* face of the secondary (daughter) lamellae growing on the *ac* face of the primary (parent) lamellae.[10] The branching angle between the two lamellae of about 80° derives from the requirement for interdigitation of methyl groups of isochiral layers. The pitch of the iPP helix and the interhelix spacing are closely similar.

A similar experimental and modeling approach has now been used to study the morphology of iPP γ transcrystallinity produced under high pressure. The crystal structure of γ iPP was fully elucidated in the late 1980s[11−15] although it was first identified almost 30 years earlier.[16] The unit cell is orthorhombic with $a = 8.54$ Å, $b = 9.93$ Å, and $c = 42.41$ Å.[11] The dimensions of the unit cell in reciprocal space are $a^* = 0.117$ Å^{-1}, $b^* = 0.101$ Å^{-1}, and $c^* = 0.0236$ Å^{-1}. The unusual feature of this polymorph is that the chain axes are not all parallel to each other but rather pairs of antichiral helices are parallel alternatively to each diagonal of the *ab* plane. Consequently, the growth direction of the γ lamellae must be assumed to coincide with the *c* axis.[14] The only published model of γ transcrystallinity, developed on Kevlar 29 and pitch-based carbon fibers, involves a mixture of α and γ forms. A unique orientation of the γ iPP crystals, consistent with the known epitaxial relationship between the γ *ab* face on the α *ac* face, was established.[8] Branching of γ iPP crystals on γ iPP is not believed to occur.

Experimental Section

Isotactic polypropylene was supplied by ExxonMobil Corp. and had M_n and M_w values of 43 600 and 212 500, respectively (melt flow rate = 12). It was made with a Ziegler Natta catalyst and has 95% *m*-pentads. (These data were provided by ExxonMobil.) The aramid Kevlar 149 fibers were provided by DuPont and had a diameter of 12 μm. The details of the preparation of the γ iPP composite under a pressure of 2500

† The Hebrew University of Jerusalem.
‡ Department of Materials and Interfaces, The Weizmann Institute of Science.
§ Chemical Services Unit, The Weizmann Institute of Science.
⊥ ESRF.
ExxonMobil Research and Engineering.
* Corresponding author: Fax 972-2-658 60 68; E-mail eric@vms.huji.ac.il.

10.1021/ma0114133 CCC: $22.00
Published on Web 12/11/2001

bar and subsequent slicing to 50 μm thick disks are reported in ref 9. As can be seen in Figure 2 of ref 9, the volume fraction of fibers is very low (a few percent), compared to the samples where a mixture of α and γ transcrystallization was induced at atmospheric pressure (weight fraction about 94%).[8]

X-ray diffraction measurements were performed at the ID11 beamline of the European Synchrotron Radiation Facility (ESRF). The beam was monochromatized (λ = 0.25 Å) and focused with a Laue crystal to 8 μm in the direction normal to the fiber and confined by a slit to 40 μm in the direction parallel to the fiber. The beam was perpendicular to the plane of the film. The exposure time was 60 s. The data were collected using a tapered-optics CCD camera (Medoptics, Tucson, AZ) with a pixel size 50 μm × 50 μm. The images were processed using the public domain NIH Image or ImageJ image processing programs, both available at zippy.nimh.nih.gov.

For scanning electron microscopy, the samples were etched[17] and then coated with a thin (20 Å) layer of chromium before observation in the JEOL field emission SEM, operated at 3.0 kV accelerating voltage. The electron beam was perpendicular to the plane of the iPP film.

Results

Scanning electron micrographs of the γ iPP tc layer developed on a Kevlar 149 fiber are shown at two different magnifications in Figure 1. Figure 1a is a picture of the transcrystalline layer nucleating at the fiber. The thickness is not uniform, probably due to temperature gradients in the crystallization cell. Figure 1b gives more details of the lamellar morphology. The lamellae appear to grow radially out from the fiber, and some disorientation of the growth direction of the lamellae with respect to the horizontal (equatorial) plane is evidenced.

In the X-ray diffraction experiments, the tc layer was sampled at 8 μm intervals in the direction approximately perpendicular to the fiber axes. Because of the nature of the preparation method,[9] the fibers could not be aligned exactly parallel to each other. In all, 20 diffraction patterns were measured, in which were included two fibers. Three patterns are shown in Figure 2, with corresponding indexing presented in Table 1. The series of X-ray diffraction patterns sampling the whole thickness of a tc layer confirms the purity of the γ transcrystallinity generated since neither the strong 130 reflection of α iPP (d = 4.78 Å) nor the 110 reflection of β iPP (d = 5.51 Å) is observed. Yet, the azimuthal positions of the center of some of the reflection arcs (measured in the upper hemisphere), reported in Table 1, vary as a function of the distance from the fiber. The azimuthal angle of reflection 117 moves progressively from 62° (Figure 2a) to 48° (Figure 2c). Near the fiber, the 026 reflection is a very broad arc centered at the equator. With increasing distance from the fiber, the reflection splits and the azimuthal angle tends to the value 34°. Reflection arcs 111 and 202 become shorter further from the fiber but appear to remain centered at the meridian; they consist of unresolved pairs. The 008 reflection is consistently equatorial. The relative intensities of the arcs also vary with distance from the fiber. The 008 and 117 reflections appear stronger further away from the fiber (Figure 2b,c) as compared to nearer the fiber surface (Figure 2a). In Figure 2a, two additional equatorial arcs, due to the diffraction of the Kevlar fiber, can be observed: these are reflections 110 (d = 4.32 Å) and 200 (d = 3.93 Å). X-ray diffraction patterns of bulk γ iPP prepared under the same conditions as the γ iPP transcrystallinity consist of rings of uniform intensity (data not shown).

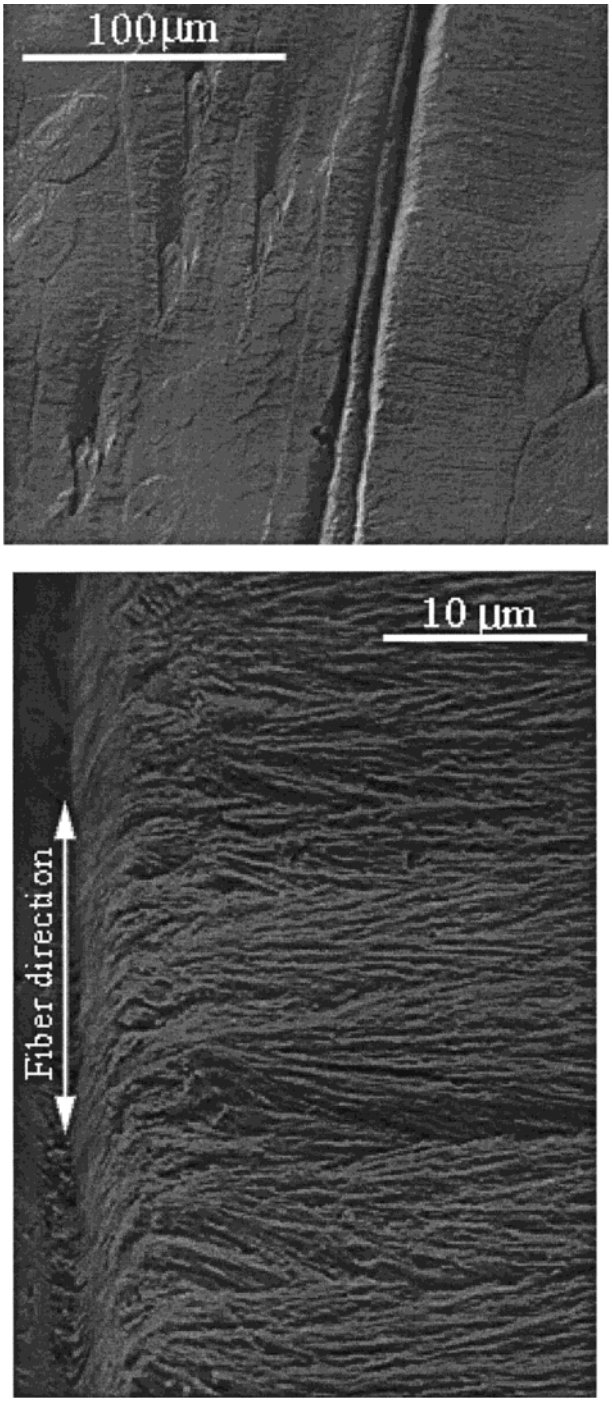

Figure 1. Low (a, top) and high (b, bottom) resolution scanning electron micrographs of a longitudinal section of the γ iPP tc layer developed on a Kevlar 149 fiber as described in ref 9. The electron beam is perpendicular to the plane of the composite.

Discussion

Model of Lamellar Orientation. The SEM micrographs of Kevlar 149/γ iPP composites prepared at high pressure establish that in the tc layer the growth axes (i.e., the c axes) extend radially outward from the surface of the aramid fiber. The X-ray diffraction patterns are consistent with this finding as the 008 reflection is always equatorial. Therefore, the lamellar ab plane must be tangential to the fiber. However, we have been unable to find a unique orientation of a and b axes with respect to the fiber axis which can explain

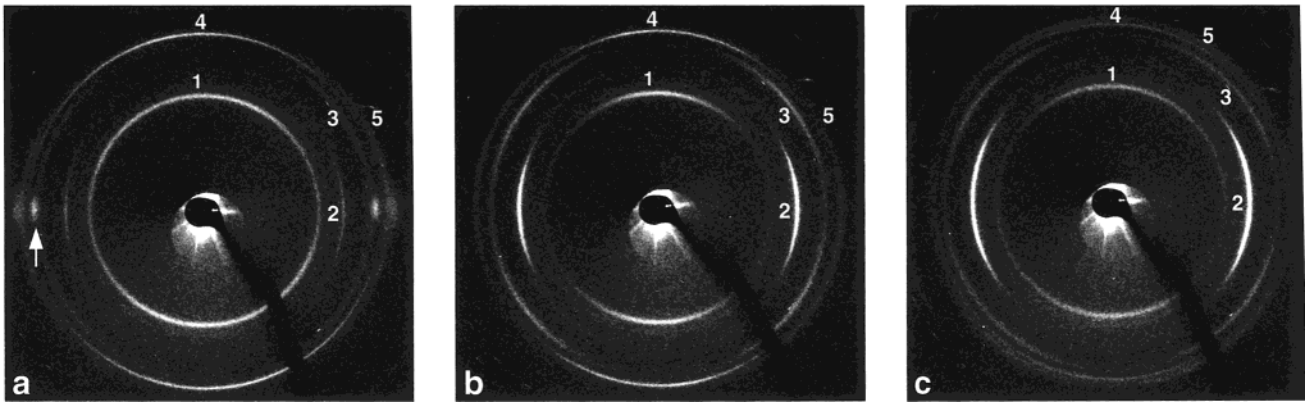

Figure 2. X-ray diffraction patterns of γ iPP transcrystallinity: (a) initial position near the surface of the first fiber (the arrow denotes the presence of the diffraction arcs of the aramid fiber); (b) 24 μm from the initial position; (c) approximately 80 μm from the second fiber. Fiber direction approximately vertical. The X-ray beam is perpendicular to the plane of the sample and has a cross-sectional area of 8 μm × 40 μm. The numbering refers to Table 1.

Table 1. Indexing of Reflections and Measured Azimuthal Angles with Respect to the Fiber Axis of the Intensity Maximum for Reflections hkl for Different Distances from the Fiber

reflection	d spacing (Å)	hkl	ϕ_{hkl} (deg) in Figure 2a	ϕ_{hkl} (deg) in Figure 2b	ϕ_{hkl} (deg) in Figure 2c
1	6.38	111	~0[a]	~0[a]	~0[a]
2	5.32	008	90	90	90
3	4.43	117	~62	~50	~48
4	4.16	202	~0[a]	~0[a]	~0[a]
5	4.06	026	~90[a]	~90[a]	~34

[a] Unresolved peak.

the various azimuthal positions of the observed X-ray reflections. Introducing lamellar twisting or sheafing into the single orientation model does not improve the agreement. Rather, the X-ray diffraction patterns of Figure 2 are consistent with a random orientation of the *ab* face of the γ iPP lamellae on the fiber surface, as schematically drawn in Figure 3. Changes in the position of the reflections with distance from the fiber can be attributed to changes in the X-ray beam sampling of the distribution of orientation of the lamellae around the fiber. This effect can be explained in the following way.

A relationship between χ, the angle between the lamella growth axis and the direction of the X-ray beam (Figure 4), and the resulting azimuthal position ϕ_{hkl} of the *hkl* reflection can be derived for random orientation of the crystallite *ab* face on the fiber surface (see Appendix):

$$\cos \phi_{hkl} = \frac{\sqrt{\mathrm{OE}^2 - (lc^*)^2/\sin^2 \chi}}{\mathrm{OE}} \qquad (1)$$

where OE is the length of the reciprocal lattice vector corresponding to reflection *hkl*:

$$\mathrm{OE} = \sqrt{(ha^*)^2 + (kb^*)^2 + (lc^*)^2} \qquad (2)$$

Crystallite *c* axes are assumed to be constrained to lie perpendicular to the fiber axis and to be distributed uniformly around the fiber. In Figure 5 are drawn the azimuthal distributions of the five observed reflections, calculated using eq 1. The calculation shows that as the angle χ between the *c* axis of a lamella, i.e., the growth direction and the X-ray beam increases from 0 to 90°, the corresponding reflection peak moves closer to the

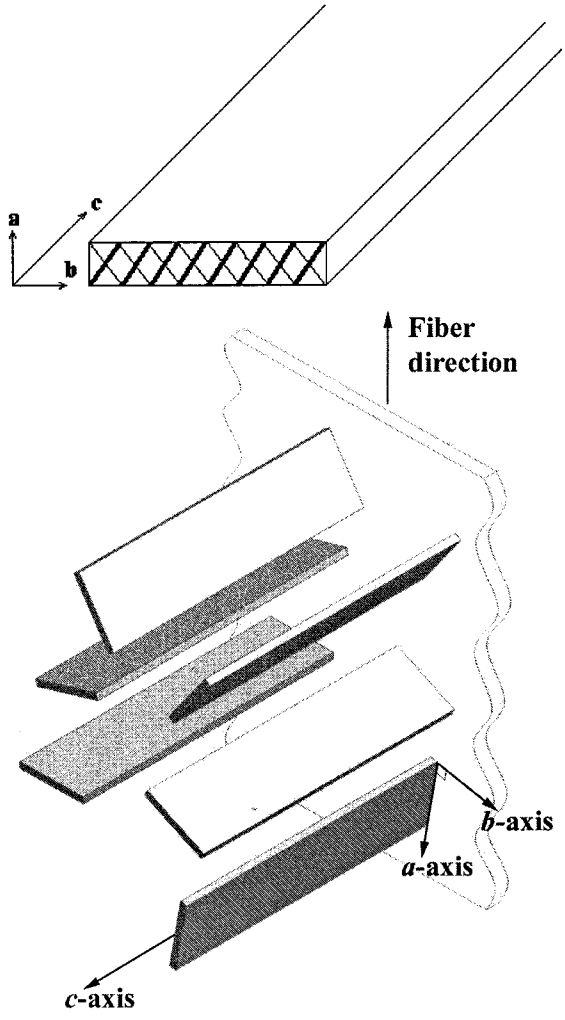

Figure 3. (a, top) Schematic drawing of a lamella of γ iPP. The heavier lines indicate polymer chains in the plane of the paper. The thinner lines indicate the chains which lie *c*/8 below the plane of the paper. (b, bottom) An idealized model of the γ iPP transcrystallinity. The *ab* planes of the lamellae are randomly oriented on the fiber surface.

meridian. Contributions to the intensity from the lamellae with small χ are distributed sparsely in the azimuthal direction whereas contributions from lamellae with large χ tend to be concentrated. When the X-ray beam is focused on or near the fiber, it samples a wide

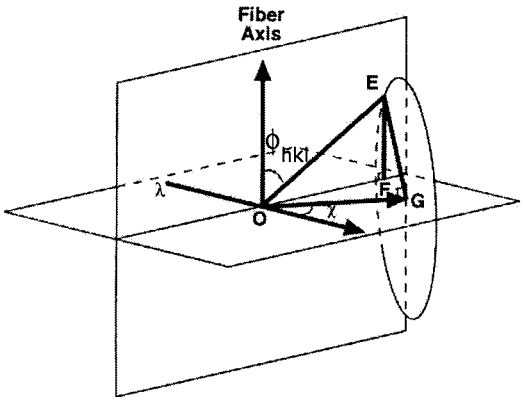

Figure 4. Geometry of X-ray diffraction from the γ iPP transcrystalline layer. The fiber is vertical. $\overline{OE}$ is one of a set of reciprocal lattice vectors of a γ iPP crystallite. c^* and the X-ray beam (λ) lie in the equatorial plane. c^* makes an angle χ with the X-ray beam. There is random orientation of a^*b^* about the c^* axis. Therefore, a circle of vectors is drawn out with radius $EG = \sqrt{(ha^*)^2+(kb^*)^2}$. The circle intersects the Ewald sphere (approximated here as a plane) at E. $\overline{OF}$ is the projection of $\overline{OE}$ on the equatorial plane. The azimuthal angle ϕ_{hkl} is the angle between the fiber axis and $\overline{OE}$.

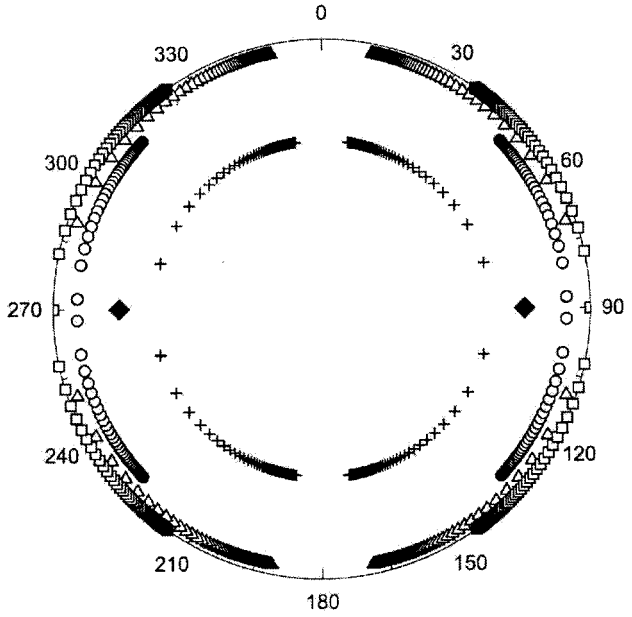

Figure 5. Azimuthal distribution of the five observed reflections calculated using eq 1. The c axes of the γ iPP crystallites are assumed to lie perpendicular to the fiber axis and to be distributed uniformly around the fiber. The ab plane has no preferential orientation about the c axis. The fiber axis is vertical. (+) 111, (◆) 008, (○) 117, (△) 202, and (□) 026.

distribution of lamellar positions, with those lamellae having c axes parallel or close to parallel to the beam likely overrepresented. In the case of $\chi = 0°$, the ab plane lies tangent to the Ewald sphere. Since c^* is much smaller than a^* and b^*, a slight disorientation of the ab plane with respect to the fiber surface makes possible the intersection of the 111 and 202 reciprocal vectors with the Ewald sphere for any orientation of the a^* and b^* axes. The reflections that are expected are therefore weak but isotropic. The 008, 117, and 026 reciprocal vectors cannot intersect the Ewald sphere because the c^* component is too large. For $0° < \chi \ll 90°$, reflections (aside from 008) will be diffused, with an emphasis on near-equatorial intensity for the 117 and 026 reflections.

Table 2. Comparison of the Predicted and Measured Azimuthal Angles with Respect to the Fiber Axis of the Intensity Maximum for Reflections *hkl* When the Lamellae Are Predominantly Perpendicular to the X-ray Beam ($\chi \sim 90°$)

reflection	indexing	ϕ_{hkl} (deg) from eq 4	ϕ_{hkl} (deg) in Figure 2c
1	111	8.7	~0[a]
2	008	90	90
3	117	46.7	~48
4	202	11.4	~0[a]
5	026	35	~34

[a] Unresolved peak.

As the X-ray beam is focused further away from the fiber, a larger fraction of lamellae lie perpendicular or close to perpendicular to the beam, and therefore the intensity maxima (aside from 008) move closer to the meridian and become sharper. In the simple case of $\chi = 90°$, the c axes of the lamellae are contained in the plane of the film. The hkl vectors lie on the circle of radius

$$EG = \sqrt{(ha^*)^2 + (kb^*)^2} \tag{3}$$

which is at a distance lc^* from the origin. The predicted azimuthal angles ϕ_{hkl}, presented in Table 2 for the case of $\chi = 90°$, are given by

$$\tan \phi_{hkl} = lc^*/EG \tag{4}$$

If all lamellae lay perpendicular to the fiber axis, the 008 reflection would be perfectly equatorial, and only those lamellae at 90° to the X-ray beam would contribute to it. However, a disorientation arc associated with 008 of width about 30° is observed. Such a distribution is also observed in the SEM micrograph (Figure 1b). In fact, each point of the four other calculated azimuthal distributions should be convoluted with a similar disorientation arc. This process would further smear the calculated azimuthal distributions; in particular, there would not be gaps at the meridian for the 111 and 202 reflections, and the 026 reflection would be even broader than it is in Figure 5. Presumably, were the nucleation density of γ-iPP higher on the Kevlar fiber, the azimuthal distribution would be narrower accordingly. In a previous communication,[9] the diameter of the X-ray beam used in the experiments was large enough to simultaneously sample an average of all orientations of the γ iPP lamellae. Diffraction characteristic of lamellae distant from the fiber dominated the pattern, because of the volume effect. The conclusions presented above are consistent with the current experimental X-ray patterns and the one obtained previously with the low spatial resolution beam.

Nucleation on Kevlar 149 Fibers: γ vs α Transcrystallization. The search for epitaxial matching between a polymer and a substrate is motivated by the search for a mechanism of nucleation that can lead to a particular polymer crystallite orientation. It is usually accepted that the upper limit for the misfit of the periodicities of the atoms in the contact lattice planes of substrate and overgrown material is about 10−15%.[18]

In a study of the structure of γ iPP thin films grown on α iPP deposited on glass,[13] two orientations were reported: (i) one with a set of the γ chain axes parallel to the α chain axes: then the angle between the γ lamellae and the α lamellae is about 40°; (ii) one with

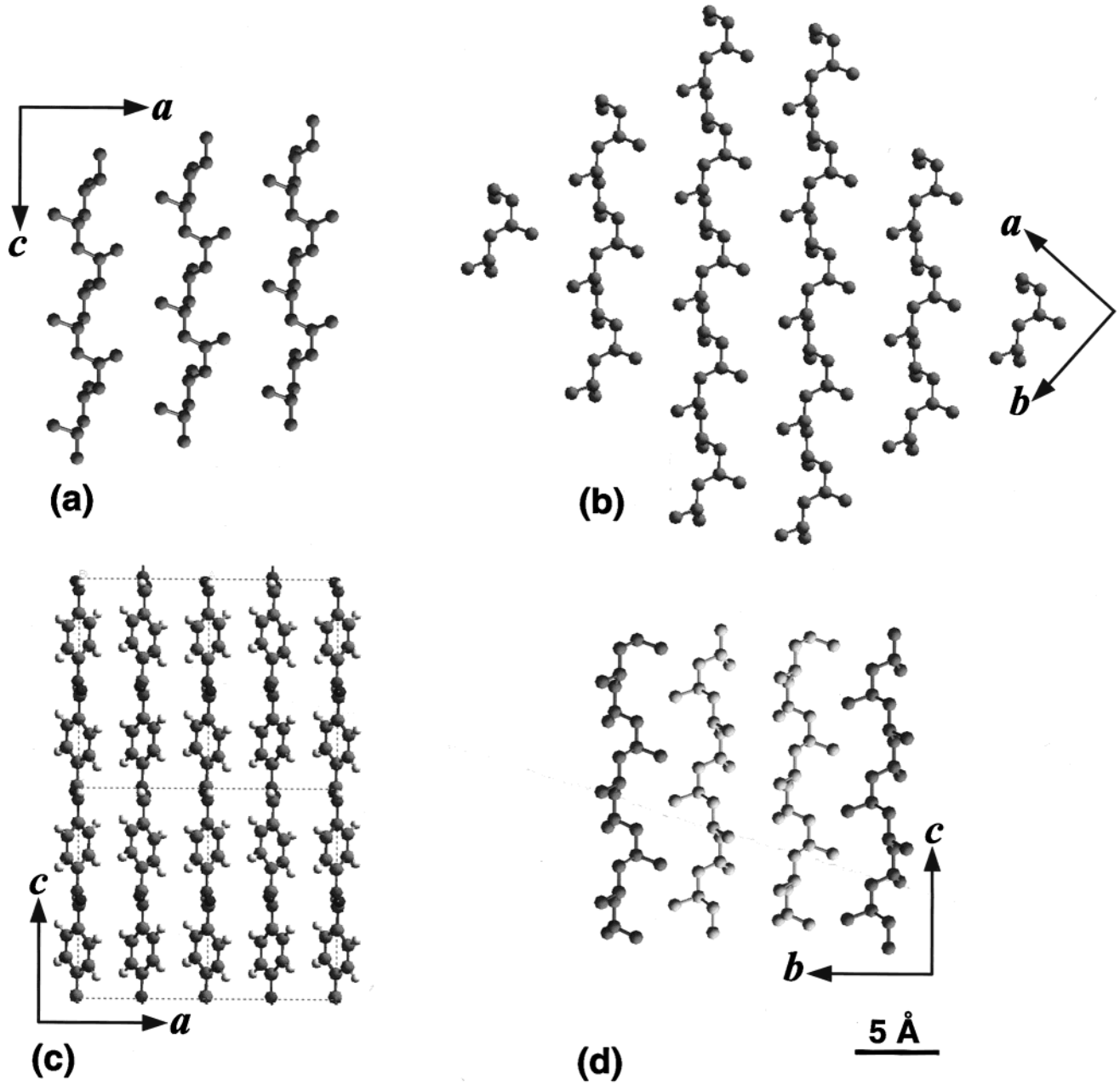

Figure 6. (a) Crystal structure of the *ac* face of α iPP. Interchain spacing is 6.65 Å. The chains are homochiral. This face is involved in the branching (homoepitaxy) and in α/γ epitaxy. (b) Crystal structure of the *ab* face of γ iPP. Interchain spacing is 6.46 Å. The chains are homochiral. Either one or two of the three methyl groups per turn of the iPP helix point out of the face. (c) Crystal structure of the *ac* face of Kevlar. Interchain spacing is 7.80 Å. There are two differently oriented aromatic rings per axial repeat unit, with $c = 12.9$ Å, which is very close to twice the pitch of the iPP helix. (d) A view of α iPP crystal structure along the direction perpendicular to the *bc* face. The molecules that are shaded darker lie in the plane of the paper. Those that are shaded lighter lie at a distance *a*/2 below the plane of the paper. The spacing between coplanar chains is alternatively 5.24 and 15.72 Å.

the γ lamellae lying with the *a* axis parallel to the glass surface and the *b* axis parallel to the α chain axis. As noted above, it has been shown that γ iPP crystallites grow on α iPP crystallites through epitaxial matching involving the γ *ab* face and the α *ac* face.[13] Indeed, the respective iPP chains are then parallel, and the distances between adjacent iPP chain axes in the two polymorphs are very similar: 6.65 Å for α iPP and 6.47 Å for γ iPP (less than 3% mismatch), as shown in Figure 6a,b.

Epitaxial nucleation of α iPP crystallites on Kevlar fibers also appears likely. Previous studies have shown that in the tc layer the *bc* planes of the parent α iPP crystallites lie tangent to the Kevlar fiber.[4,5] According to the core-skin structure of Kevlar, the *ab* planes of its orthorhombic lattice ($a = 7.80$ Å, $b = 5.19$ Å, and $c = 12.9$ Å) are directed radially from the fiber axis.[19] Therefore, the crystal face that is in contact with the nucleating iPP is the *ac* face. Figure 6c,d shows the crystal structures of the *ac* plane of the Kevlar fiber and the *bc* face of α iPP. It is seen in Figure 6d that at the *bc* surface of the unit cell the distance between neighbor α iPP chains is alternatively 5.24 and 15.72 Å. The superposition of Figure 6c,d with the chain axes of the Kevlar fiber aligned parallel to those of the α iPP chains shows an epitaxial matching: $b_{\alpha iPP} \sim 3a_{Kevlar}$ with a mismatch about 10% and $2c_{\alpha iPP} \sim c_{Kevlar}$ with a mismatch about 3%. It is noted that epitaxial growth of α

iPP on a substrate was found to involve the 010 or the 110 contact face[20] and not the *bc* plane as suggested here. Yet, the mismatch between the *ac* face of α iPP and the *ac* plane of the Kevlar fiber would be greater, about 15%. Moreover, steric hindrances would be more stringent because the aromatic rings would have to be inserted in between close-packed iPP chains. The proposed epitaxial matching between the *bc* face of α iPP and the *ac* plane of the Kevlar fiber may explain the observation of a unique orientation of the α iPP lamellae at the surface of the Kevlar fiber.

In the case of γ transcrystalline iPP, the *c* axis is the lamellar growth direction. Although there is no direct evidence, the *c* axis is also most likely perpendicular to the fiber surface at the nucleation stage. Indeed, the direction of the deposition of the polymer chains is perpendicular to the *ab* plane. Therefore, the *ab* plane of the γ iPP crystals must be in contact with the external face of the Kevlar fiber, i.e., the *ac* face of the Kevlar crystals.[19] According to the crystal structure of γ iPP,[10] every third methyl group or two out of three methyl groups of the chains lying in the *ab* plane face out toward the *ac* face of the Kevlar fiber. Since the faces that are in contact are fixed, possible epitaxy was considered by rotation of the *a* and *b* axes of the γ iPP unit cell about the *c* axis. No satisfactory matching could be found. For instance, for the epitaxial matching similar to that considered for the two conformations described above,[13] the two-dimensional lattice mismatch is too large to be acceptable. In the direction perpendicular to the Kevlar chains, it is about 17% and 10% for conformations in which the Kevlar chains are either parallel to one set of γ iPP chains or bisect the two sets of γ iPP chains, respectively. In the direction perpendicular to the Kevlar chains, it is approximately 3% and 23%, respectively. These calculations take into account only the lattice constants but not the steric hindrance due to the rings in the Kevlar molecules. Hence, the true epitaxial matching can be only less satisfactory, and it is probable that the nucleation is not epitaxial. Therefore, it is concluded that in the absence of a preferential interaction at the fiber surface a random orientation of the *ab* face of the γ crystals on the Kevlar fiber is most probable. In an earlier study,[8] where a mixture of α and γ transcrystallinity was generated at atmospheric pressure on the surface of either Kevlar 29 or carbon fibers, a unique orientation for the γ lamellae was found (i.e., the *a* axis makes an angle of 40.7° with the fiber axis). As noted above, it was established in spherulitic iPP that the *ab* face of γ lamellae grows epitaxially on the *ac* face of α lamellae (both parent and daughter lamellae). It is therefore likely that this type of epitaxy occurs in their composites and fixes the orientation of the γ phase with respect to the oriented α lamellae in the tc layer. Hence, the presence of the α phase does not allow a random positioning of the *ab* plane of the γ crystallites with respect to the fiber axis.

Conclusions

Some central features of the morphology of γ iPP transcrystallinity on Kevlar aramid fibers have been elucidated. SEM micrographs of the γ tc layer and microbeam X-ray diffraction support the idea that the lamellae nucleate at the fiber surface and then grow radially with the *c* axis parallel to the growth direction. It was also established that the *ab* face of a γ iPP crystallite in contact with the fiber surface has no preferred orientation with respect to the fiber axis. The model is fully consistent with the X-ray patterns obtained at both low and high spatial resolution experiments. It also takes into account the orientational distribution of the lamellae with respect to the X-ray beam. No epitaxial relationship between the *ac* face of the Kevlar crystallites and the *ab* face of the γ iPP crystallites could be found, thereby supporting the idea of random orientation of the *ab* face of the γ iPP crystals on the fiber surface.

Acknowledgment. H.D.W. is the recipient of the Livio Norzi Professorial Chair. This project was supported by a grant from the MINERVA Foundation and by the Israel Ministry of Science. The authors thank Dr. René Fulchiron (Université Lyon I) for his valuable help in the use of the PVT apparatus to generate γ iPP transcrystallinity; Bill Lamberti (ExxonMobil Corporate Strategic Research) for the scanning electron micrographs (Figure 1), Dr. Isabelle Weissbuch (Weizmann Institute of Science) for the molecular drawings (Cerius2, Figure 6), and Beni Pasmantirer (Weizmann Institute of Science) for the drawing of Figures 3 and 4.

Appendix: Derivation of the Relationship between γ IPP Lamellar Orientation and the Diffraction Pattern Azimuthal Angles ϕ_{hkl}

The azimuthal angle ϕ_{hkl} is the angle the reciprocal lattice vector associated with a given reflection (*hkl*) makes with the fiber axis, as illustrated in Figure 4. Since for all observed reflections $\cos\theta \sim 1$, where θ is the Bragg angle, the Ewald sphere can be considered locally as a plane. *a***b** axes are randomly oriented about the *c** axis; out-of-plane disorientation of the crystallite *c* axes of γ iPP is neglected. When the *c** axis of a γ iPP crystallite makes an angle $0° \leqslant \chi \leqslant 90°$ with the X-ray beam direction, the locus of reciprocal lattice vectors *hkl* describes a circle which intersects the Ewald sphere at the point E. $\overline{OF}$ is the projection of $\overline{OE}$ on the equatorial plane. Thus, ϕ_{hkl} is defined by

$$\cos\phi_{hkl} = EF/OE \tag{5}$$

where OE is the length of the reciprocal vector associated with the reflection (*hkl*):

$$OE = \sqrt{(ha^*)^2 + (kb^*)^2 + (lc^*)^2} \tag{2}$$

The angle χ is given by

$$\sin\chi = OG/OF \tag{6}$$

with

$$OG = lc^* \tag{7}$$

and

$$EG^2 = OE^2 - OG^2 \tag{8}$$

Thus

$$\cos\phi_{hkl} = \frac{\sqrt{OE^2 - (lc^*)^2/\sin^2\chi}}{OE} \tag{1}$$

References and Notes

(1) Petermann, J. In *Polypropylene Structure, Blends and Composites*, 1st ed.; Karger-Kocsis, J., Ed.; Chapman & Hall: London, 1995; Vol. 1, p 140.

(2) Stern, T.; Wachtel, E.; Marom, G. *J. Polym. Sci., Part B: Polym. Phys.* **1997**, *35*, 2429−2433.
(3) Chen, E. J. H.; Hsiao, B. S. *Polym. Eng. Sci.* **1992**, *32*, 280−286.
(4) Assouline, E.; Wachtel, E.; Grigull, S.; Lustiger, A.; Wagner, H. D.; Marom, G. *Polymer* **2001**, *42*, 6231−6237.
(5) Dean, D. M.; Rebenfeld, L.; Register, A.; Hsiao, B. S. *J. Mater. Sci.* **1998**, *33*, 4797−4812.
(6) Varga, J.; Karger-Kocsis, J. *Polymer* **1995**, *36*, 4877−4881.
(7) Assouline, E.; Pohl, S.; Fulchiron, R.; Gérard, J.-F.; Lustiger, A.; Wagner, H. D.; Marom, G. *Polymer* **2000**, *41*, 7843−7854.
(8) Dean, D. M.; Register, R. A. *J. Polym. Sci., Part B: Polym. Phys.* **1998**, *36*, 2821−2827.
(9) Assouline, E.; Fulchiron, R.; Gérard, J.-F.; Wachtel, E.; Wagner, H. D.; Marom, G. *J. Polym. Sci., Part B: Polym. Phys.* **1999**, *37*, 2534−2538.
(10) Padden, J. F., Jr.; Keith, H. D. *J. Appl. Phys.* **1966**, *37*, 4013−4020.
(11) Bruckner, S.; Meille, S. V. *Nature* **1989**, *340*, 455−457.
(12) Meille, S. V.; Bruckner, S.; Porzio, W. *Macromolecules* **1990**, *23*, 4114−4121.
(13) Lotz, B.; Graff, S.; Straupé, C.; Wittmann, J. C. *Polymer* **1991**, *32*, 2902−2910.
(14) Thomann, R.; Wang, C.; Kressler, J.; Mülhaupt, R. *Macromolecules* **1996**, *29*, 8425−8434.
(15) Angelloz, C.; Fulchiron, R.; Douillard, A.; Chabert, B.; Fillit, R.; Vautrin, A.; David, L. *Macromolecules* **2000**, *33*, 4138−4145.
(16) Morrow, D. R. *J. Appl. Phys.* **1968**, *39*, 4944−4950.
(17) Bassett, D. C.; Olley, R. H. *Polymer* **1984**, *25*, 935−943.
(18) Wittmann, J. C.; Lotz, B. *Prog. Polym. Sci.* **1990**, *15*, 909−948.
(19) Yang, H. H. In *Kevlar Aramid Fiber*; Chapman & Hall: London, 1993; p 71.
(20) Mathieu, C.; Thierry, A.; Wittmann, J. C.; Lotz, B. *Polymer* **2000**, *41*, 7241−7253.

MA0114133